

Zircon formation from amorphous spherical ZrSiO_4 particles obtained by hydrolysis of aerosols

P. TARTAJ, J. SANZ, C. J. SERNA, M. OCAÑA

Instituto de Ciencia de Materiales, CSIC, Serrano 115 dpdo, 28006 Madrid, Spain

A procedure for the preparation of $\text{SiO}_2 \cdot \text{ZrO}_2$ spherical particles, based on the hydrolysis of liquid aerosols is described. A mixture of tetraethylortho-silicate (TEOS) and zirconium *n*-propoxide with the proper stoichiometry (Zr/Si atomic ratio = 1) was used as a liquid precursor. The alkoxide mixture had to be partially hydrolysed before aerosol generation in order to obtain solids with a zircon composition. The as-prepared powders consisted of particles in the micrometre range with an amorphous character. Energy dispersive X-ray spectroscopy (EDX), infrared (i.r.) and nuclear magnetic resonance (NMR) analyses indicated the existence of a good compositional homogeneity and a large number of Si–O–Zr bonds in the sample. Calcination of the powder up to 950 °C gave rise to the segregation of silica and the crystallization of tetragonal zirconia, which transformed into the monoclinic phase after heating at 1300 °C. Crystallization of zircon started on calcination at 1450 °C; it was accompanied by the formation of some cristobalite. The complete transformation of the sample into zircon took place after prolonged heating (20 h) at 1500 °C.

1. Introduction

High-purity and non-agglomerated powders with controlled particle size and a spherical shape are highly desirable for ceramic processing. Zircon (ZrSiO_4) is an important ceramic material due to its high resistance to thermal shock and its low thermal expansion. Recently, zircon powders have been synthesized by the sol–gel route [1–3], which yielded heterogeneously shaped particles [1–3], and agglomerated solids [3]. Spray pyrolysis techniques [4–7] have also been used, producing spherical $\text{SiO}_2 \cdot \text{ZrO}_2$ particles, although, in some cases, the spheres obtained were hollow and crushed [7]. Recently, it has been shown that non-hollow amorphous spherical particles of multicomponent oxides can be synthesized by room-temperature hydrolysis of liquid aerosols containing alkoxides or other hydrolysable precursors [8–11]. However, in this method, the fact that each starting compound has, in general, a different hydrolysis rate makes it very difficult to control the stoichiometry of the resulting powders [8, 9, 11] and this can produce an important compositional heterogeneity inside the particles [8, 9].

In the present work, the preparation of non-hollow and non-agglomerated ZrSiO_4 amorphous spherical particles by hydrolysis of aerosols generated from mixtures of tetraethylorthosilicate and zirconium *n*-propoxide is reported. The control of the stoichiometry of the powders was carried out by partially hydrolysing the alkoxide mixtures before the aerosol generation; this led to a good degree of chemical

homogeneity in the particles. The thermal evolution of the powders so obtained, up to the crystallization of zircon, was studied by differential thermal analysis (DTA), thermogravimetric analysis (TGA), X-ray diffraction (XRD), infrared (i.r.) spectroscopy and ^{29}Si nuclear magnetic resonance (NMR).

2. Experimental procedure

2.1. Preparation of the powders

The method described here for the preparation of the zircon powders consists of the generation of an aerosol from hydrolysable liquid precursors and subsequent hydrolysis to form the corresponding oxide. Spherical particles are always produced since the liquid droplets behave as separate reactors. The particle-size distribution is determined by the characteristics of the aerosol generator.

Zirconium *n*-propoxide (Aldrich, technical grade) and tetraethylorthosilicate (TEOS, Fluka, 98%) were used as starting compounds. The as-supplied alkoxides were first quickly mixed at 20 °C under magnetic stirring with the Zr/Si atomic ratio equal to unity. The mixture was then nebulized and hydrolysed at 20 °C in the apparatus schematically represented in Fig. 1; this apparatus is slightly modified from an apparatus previously used for mullite preparation [11]. The nebulization of the starting liquid into the expansion chamber was carried out by using a glass nozzle with nitrogen at a constant pressure (0.3 kg cm^{-2}) as the carrier gas. The resulting aerosol was then hydrolysed with water

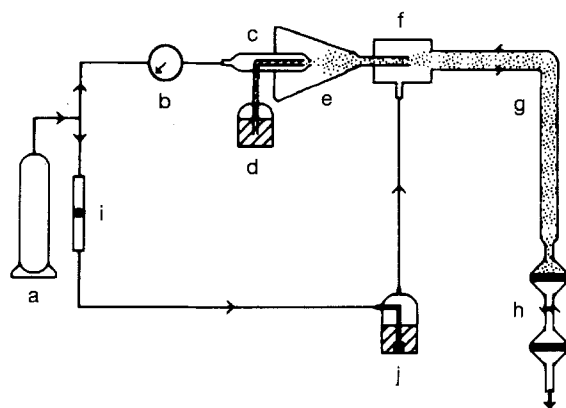


Figure 1 A schematic diagram of the apparatus used to produce $\text{SiO}_2 \cdot \text{ZrO}_2$ spherical particles: (a) N_2 tank, (b) manometer, (c) glass nozzle, (d) starting-liquid container, (e) expansion chamber, (f) injection manifold, (g) hydrolysis chamber, (h) nylon sieves, (i) flowmeter, and (j) bubbler.

vapour brought into contact with the aerosol stream by bubbling nitrogen at a constant flow rate (2 l min^{-1}), through a water container (j). The particles so produced were collected by using a system of nylon sieves.

In most experiments, the starting alkoxide mixture was partially hydrolysed before the aerosol generation. For such purposes, the mixture was placed in a beaker (100 cm^3) with a resulting liquid surface/volume ratio of 0.65 cm^{-1} , and it was kept under magnetic stirring at 20°C in an atmosphere of 60% relative humidity, for different periods of time.

2.2. Characterization techniques

Both, scanning electron microscopy (SEM, Zeiss, DSM 960) and transmission electron microscopy (TEM, Jeol, 2000 FX2) were used to examine the morphological characteristics of the powders. Their size distribution was obtained from the TEM micrographs by counting several hundreds of particles. The chemical composition of the samples was evaluated by TEM using an EDX-type analyser (Link, QX 2000), and X-ray fluorescence (Siemens, SRS 300).

DTA and TGA (Stanton, STA 781) were carried out in air at a heating rate of $10^\circ\text{C min}^{-1}$. The formation of different crystalline phases in the solids was assessed by using XRD (Philips, PW 1710).

To record the i.r. spectra (Nicolet, 20 SXC) the samples were diluted in KBr. High-resolution ^{29}Si NMR spectra of the powders were registered at 79.5 MHz, by spinning (4000–5000 c.p.s. – cycles per second) the sample at the magic angle ($54^\circ 44'$), using a spectrometer equipped with Fourier transform unit (Bruker, MSL 400). To obtain the spectra, a $\pi/2$ pulse ($4 \mu\text{s}$) and a recycle delay of 5 s were selected. Tetramethylsilane (TMS) was used as an external standard reference.

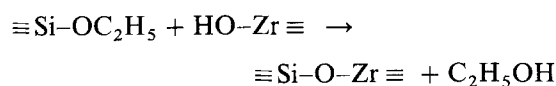
Heating of the solids was performed by keeping the samples in a furnace preheated at the desired temperature. Except when otherwise specified the calcination time was 2 h.

3. Results and discussion

3.1. Powder generation

The hydrolysis of an aerosol generated from a freshly prepared mixture of the silicon and zirconium alkoxides yielded a powder with a zirconium/silicon atomic ratio ($\text{Zr/Si} = 1.25$) higher than that of the starting mixture ($\text{Zr/Si} = 1$); (see Table I). This is attributable to the hydrolysis rate of TEOS which is much lower than that of the zirconium alkoxide. To achieve the zircon stoichiometry, some experiments were conducted with a prehydrolysis of the starting mixture at 20°C in an atmosphere of 60% relative humidity. In effect, by increasing the time of the prehydrolysis under these experimental conditions, the Zr/Si atomic ratio in the powder became lower, reaching the value corresponding to the zircon composition for a prehydrolysis time of 24 h (Table I).

In order to investigate the extension of the reaction and the nature of the species formed during the prehydrolysis process, ^{29}Si NMR spectroscopy was used. The spectra registered for the alkoxide mixtures after different prehydrolysis times are shown in Fig. 2. As observed, for the initial mixture, only one band at -82.3 p.p.m. (parts per million), corresponding to TEOS was detected. However, after 8 h of prehydrolysis, new bands at -87.0 and -87.9 p.p.m. appeared, the intensity and linewidth of these bands increased with the prehydrolysis time (20 h). These two bands cannot be due to hydrolysed TEOS since the chemical shift associated with the substitution of an ethoxide group by OH would be about $+3$ p.p.m. assuming additive substitutional effects [12]. In addition, the spectrum of pure TEOS after it had been kept for 24 h under the conditions used for prehydrolysing the mixture (at 20°C and 60% relative humidity) remained unaltered, indicating that no appreciable TEOS hydrolysis takes place during ageing. Consequently, the formation of Si–O–Si bonds can also be disregarded. From these observations, it can be concluded that the bands at -87.0 and -87.9 p.p.m. must be due to the presence of Si–O–Zr bonds produced by the following condensation reaction:



The $\text{HO-Zr}\equiv$ species would appear in the media as a result of the hydrolysis of the zirconium alkoxide

TABLE I The amount of TEOS remaining unreacted after prehydrolysing (at a temperature of 20°C and at a relative humidity of 60%) a mixture of TEOS and zirconium propoxide (with a Zr/Si atomic ratio equal to unity) for different periods of time; the chemical composition of the silica–zirconia powders obtained by hydrolysis of the aerosol which was generated from the prehydrolysed mixtures is also included

	Time (h)			
	0	8	20	24
Unreacted TEOS (%)	100	80	50	45
Zr/Si (atomic)	1.25	1.10	1.05	1.00

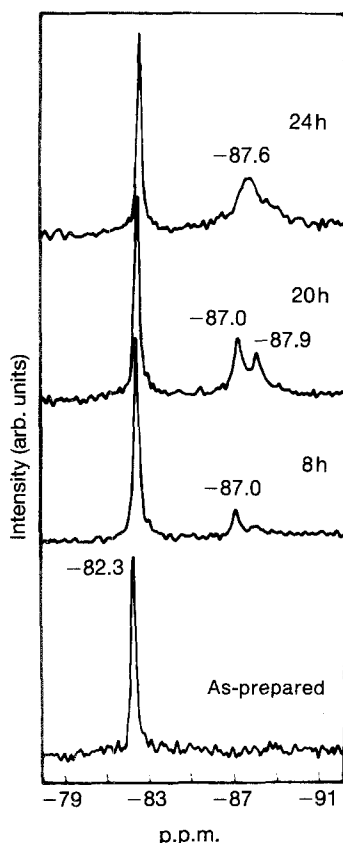


Figure 2 The ^{29}Si NMR spectra of a TEOS/zirconium *n*-propoxide mixture (Zr/Si atomic ratio = 1) in the as-prepared (initial) state and after being partially hydrolysed, for different periods of time, at 20°C in an atmosphere with a 60% relative humidity.

by moisture in the air. A similar behaviour has been observed in TEOS–aluminium–butoxide mixtures aged in humid air [13]. Longer prehydrolysis times (24 h) gave rise to a broadening of these two bands and a new maximum appeared at around -87.6 p.p.m., indicating progress in the condensation reactions giving rise to $\text{Si}(\text{OC}_2\text{H}_5)_{4-n}(\text{OZr})_n$ species, with n ranging from 1 to 3.

The relative intensity of the -82.3 p.p.m. band has been used to evaluate the amount of TEOS which remains unreacted after prehydrolysing the alkoxide mixtures. As given in Table I, at least 55% of the initial TEOS has to react with the zirconium alkoxide in order to obtain the zircon composition in the final powder.

3.2. Powder characterization

A SEM micrograph of the powder with the zircon composition (obtained under the conditions specified in the captions) is shown in Fig. 3a. The particle-size-distribution analysis (Fig. 4) gave a mean diameter of $0.63\ \mu\text{m}$. It should be mentioned that the size distribution can be altered by changing the characteristics of the aerosol generator (type of nozzle, gas-flow rates, etc).

TEM microanalysis carried out on single particles of the powder shown in Fig. 3 revealed that all of the particles had a similar composition, corresponding to the average value obtained for the powder ($\text{Zr}/\text{Si} = 1$).

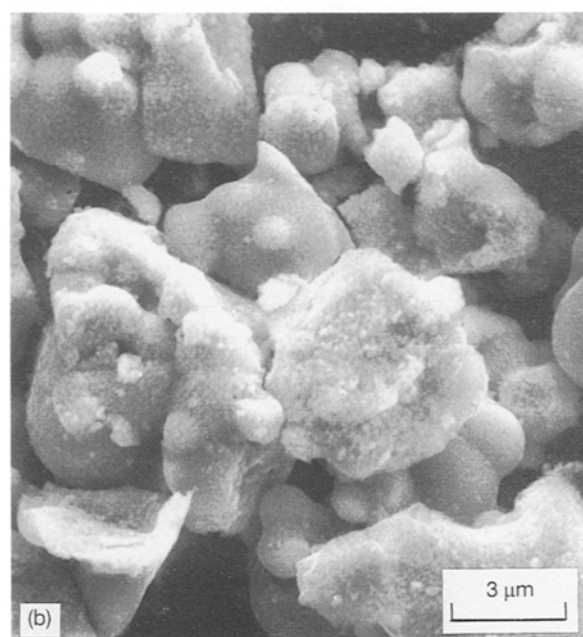
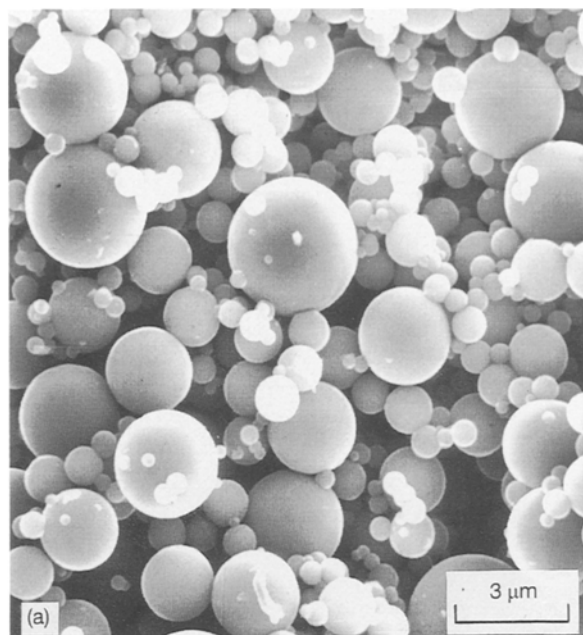


Figure 3 (a) A SEM micrograph of a $\text{SiO}_2\text{-ZrO}_2$ sample obtained by hydrolysis of an aerosol under the following conditions. The starting liquid was a mixture of TEOS and zirconium *n*-propoxide (Zr/Si atomic ratio = 1) kept for 24 h at 20°C in an atmosphere with a relative humidity of 60%. Nitrogen pressure was used to generate the aerosol, $0.3\ \text{kg cm}^{-2}$; the flow rate of the nitrogen bubbled through the water container was $2\ \text{l min}^{-1}$. (b) A SEM micrograph of the same sample heated for 2 h at 1400°C .

The same Zr/Si value was also measured when different spots within the analysed particle were considered. These results seem to indicate a high degree of compositional homogeneity in the sample.

The as-prepared spherical $\text{ZrO}_2\cdot\text{SiO}_2$ particles were amorphous to XRD. Their i.r. spectra displayed two strong absorptions at 990 and $455\ \text{cm}^{-1}$, which can be attributed to Si-O and Zr-O vibrations, respectively. In addition, the spectra also display weak bands – at 968 , 1008 and $1046\ \text{cm}^{-1}$ (Fig. 5) and at 1390 , 1455 , 2880 , 2935 and $2965\ \text{cm}^{-1}$ (not shown in Fig. 5) – due to organic impurities [14] from the

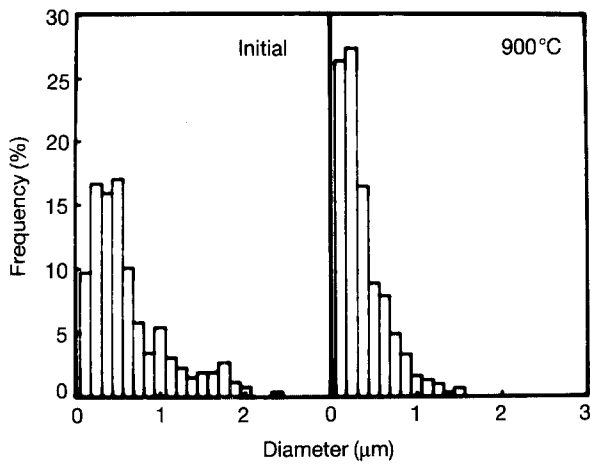


Figure 4 Particle size histograms of the sample shown in Fig. 3a, and of the same sample after being heated for 2 h at 900°C.

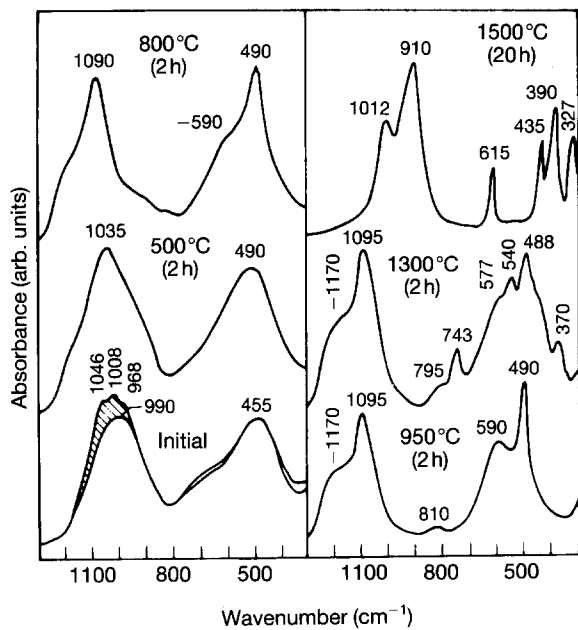


Figure 5 Infrared spectra of the sample shown in Fig. 3a in the as-prepared (initial) state and after heating at different temperatures for different periods of time. The shaded bands are due to organic impurities which can be removed by washing.

residual alkoxide groups and adsorbed alcohols generated as by-products of the hydrolysis reaction, which disappeared after washing the sample with distilled water (Fig. 5). It should be noted that the frequency of the Si–O stretching band (990 cm^{-1}) is significantly lower than the band corresponding to the same type of vibration in amorphous silica ($1200\text{--}1065\text{ cm}^{-1}$) [15]. This behaviour manifests the presence of an elevated number of Si–O–Zr bonds in the sample, supporting the good compositional homogeneity suggested by the TEM microanalysis. The same conclusion can be deduced from the ^{29}Si NMR spectrum of the sample (Fig. 6), which does not show the band at -110 p.p.m. due to amorphous silica [16], but a broad band centered at -89.3 p.p.m. is shown and it could mainly correspond to $\text{Si}(\text{OSi})_2(\text{OZr})_2$ and $\text{Si}(\text{OSi})(\text{OZr})_3$ environments. The presence of these Si–O–Si bonds in the final powder

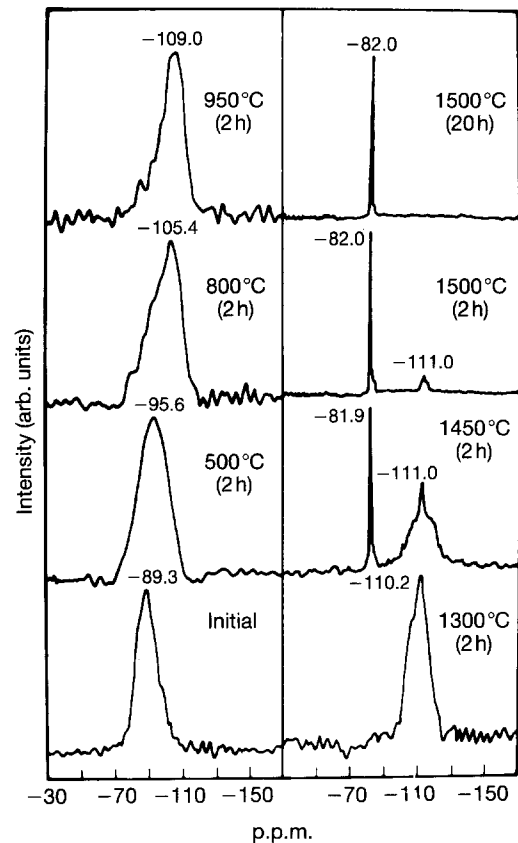


Figure 6 ^{29}Si NMR spectra of the sample shown in Fig. 3a in the as-prepared (initial) state and after heating at different temperatures for different periods of time.

would be the result of the total hydrolysis of the mixture (free TEOS + species formed during prehydrolysis) in the aerosol stream.

3.3. Thermal treatments

The DTA curve of the sample (Fig. 7) showed two strong endothermic peaks at 90 and 275°C ; they are attributed to the release of adsorbed water and alcohols. The weaker exothermic effect observed at 310°C may be due to the decomposition of the remaining organic species (residual alkoxide groups and alcohols). The total weight loss associated with these processes, measured by TGA (Fig. 7), was 35%. Finally, an additional exothermic peak appeared at 905°C in the DTA curve; the origin of this peak will be analysed in the next paragraph.

From the XRD results, the powder remained amorphous on calcination up to 900°C . During this treatment, the $\text{SiO}_2\cdot\text{ZrO}_2$ particles experienced a shrinkage (Fig. 4) as a consequence of the elimination of water and organic impurities; this resulted in a mean particle diameter of $0.38\text{ }\mu\text{m}$. After heating at 950°C (Fig. 8), the crystallization of zirconia was detected, which could account for the exothermic peak at 905°C in the DTA curve. Although the observed pattern could correspond to either tetragonal zirconia of low crystallinity or to cubic zirconia, the appearance of a band at 590 cm^{-1} in the i.r. spectrum of the sample (Fig. 5), seems to indicate the formation of the tetragonal phase [17]. The i.r. spectra of the sample

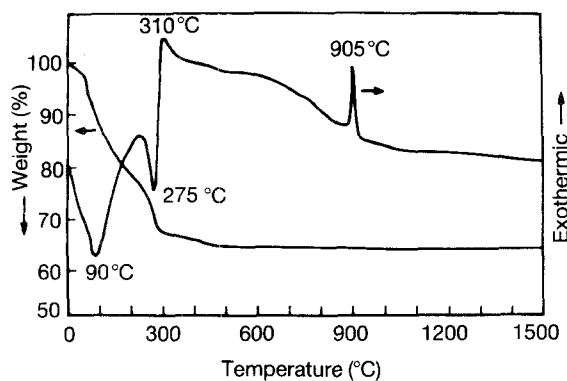


Figure 7 DTA and TGA curves for the sample shown in Fig. 3a.

heated at increasing temperatures (Fig. 5) also shows a progressive shift of the Si–O stretching mode (990 cm^{-1}) towards higher frequencies; this can be attributed to the replacement of Si–O–Zr by Si–O–Si bonds in the solid. This process ended with the segregation of silica after heating at 950°C , as manifested by the i.r. spectrum showing bands at 1170 , 1095 , 810 and 490 cm^{-1} which are characteristic of amorphous silica [15]. Additional support for this interpretation is given by the ^{29}Si NMR spectra of the sample heated between 500 – 950°C (Fig. 6) in which the -89.3 p.p.m. band progressively shifts towards the position of silica. The broadness of this component could be due to the superposition of different bands associated with chemical environments intermediate between those of silica and of the original sample. The shift in its position would be the result of the successive elimination of the Zr-rich environments as the calcination temperature increases. Similar results have been observed by Hartman *et al.* [18] during the thermal treatment of gels with a zircon composition prepared from an alkaline ($\text{pH} = 9$) aqueous medium, in which crystallization of zirconia was accompanied by segregation of amorphous silica. It should be noted that the temperature of crystallization of tetragonal zirconia in our case is much higher than that observed for pure zirconia (330°C) [17] or for other reported $\text{SiO}_2 \cdot \text{ZrO}_2$ samples (500 – 600°C) [7, 19]. Such a retarding effect should be related to the high degree of Si–Zr mixing exhibited by our sample, which implies that a segregation of the zirconia is required before its crystallization.

XRD showed the transformation from tetragonal to monoclinic zirconia after calcination at 1300°C ; it proceeded on heating at 1400°C (Fig. 8). This process, which was not manifested by the DTA results, was considerably retarded when compared with the case of pure zirconia (700°C) [17]. Similar behaviour has been previously observed by other authors and it has been explained by the blocking effect of silica, which would hinder particle growth, keeping the particle size of zirconia within its critical value in the tetragonal phase [4, 20]. The i.r. spectrum of the sample heated at 1300°C also manifested the tetragonal–monoclinic phase transformation with the apparition of bands at 743 , 540 and 370 cm^{-1} (Fig. 5) due to the monoclinic phase [17]. ^{29}Si NMR spectro-

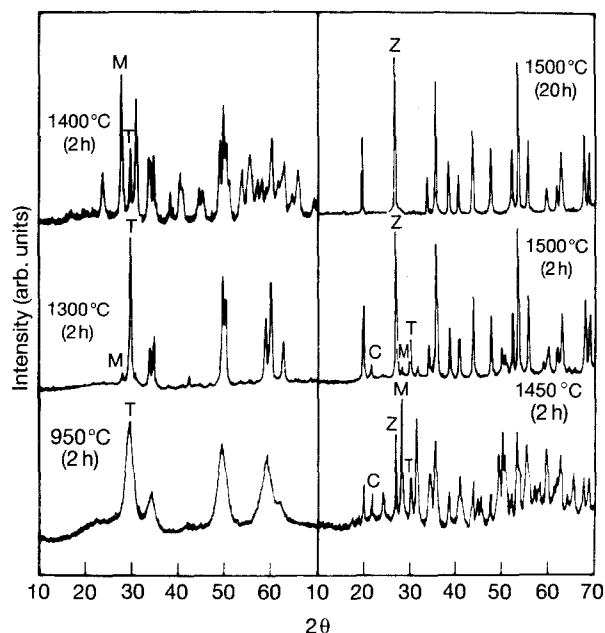


Figure 8 X-ray diffraction patterns of the sample shown in Fig. 3a after heating at different temperatures for different periods of time. The most intense reflection of each phase has been marked by the following symbols: (T) tetragonal zirconia, (M) monoclinic zirconia, (C) cristobalite, and (Z) zircon.

scopy showed that silica was completely segregated after this treatment (Fig. 6). The calcination of the powder at 1400°C gave rise to irregular particle morphologies (Fig. 3b) as a consequence of interparticle sintering.

Further heating of the solid at 1450°C , resulted in an increase in the amount of monoclinic zirconia at the expense of the tetragonal phase and of the crystallization of zircon and cristobalite (Fig. 8). In support of this, narrow bands at -81.9 and -111.0 p.p.m. appeared in the ^{29}Si NMR spectrum of the heated sample (Fig. 6); these bands were due to zircon [21] and cristobalite [18], respectively. A broad component overlapping that of cristobalite was also present in this spectrum, indicating that amorphous silica still remained in the solid. The existence of residual amorphous material after heating $\text{SiO}_2 \cdot \text{ZrO}_2$ gels in this temperature range has also been observed by Hartman *et al.* [18]. It should be noted that the temperature of zircon formation observed here (1450°C) is lower than that previously reported [4, 19, 20]; this might be explained by the good chemical homogeneity attained in our initial sample [19].

The crystallization of zircon continued at 1500°C , and this was accompanied by an important decrease in the content of monoclinic zirconia (Fig. 8), amorphous silica (Fig. 6) and cristobalite (Figs 6 and 8). However, the tetragonal-zirconia content remained unaltered during this treatment (Fig. 8). A prolonged heating (20 h) at 1500°C was necessary to complete the total transformation of the sample into zircon, as indicated by the XRD results (Fig. 8) and the NMR spectroscopy (Fig. 6). In agreement, the i.r. spectrum of the heated sample (Fig. 5) only shows the vibrational features of zircon [22].

It has been suggested that tetragonal zirconia is more favourable than the monoclinic phase for the formation of zircon from gels [1]. However, our results could indicate that zircon is preferentially formed from the monoclinic phase, since crystallization of zircon started after the beginning of the tetragonal–monoclinic transformation and it proceeded with a significant decrease of the monoclinic-phase content. High temperature X-ray diffraction experiments are being conducted in order to clarify the nature of the zirconia phase involved in the formation of zircon.

4. Conclusion

We have shown that amorphous spherical particles in the system $\text{SiO}_2\text{--ZrO}_2$, including the desired composition of $\text{SiO}_2\cdot\text{ZrO}_2$, can be prepared by room-temperature hydrolysis of aerosols consisting of mixtures of silicon and zirconium alkoxides. In order to obtain the composition of zircon, the starting alkoxide mixture had to be partially hydrolysed before the aerosol generation. The calcination of the powders yielded zircon at lower temperatures than those required for other reported synthesized samples; this is ascribed to the good chemical homogeneity (the large number of Si–O–Zr bonds) in our initial sample.

Acknowledgement

We thank Professor J. S. Moya for helpful discussions and Dr I. Sobrados for her technical assistance with the NMR spectra recording. This research was supported by the CICYT under Project MAT92-0328. One of us (P. Tartaj) acknowledges a fellowship of Spain's Ministerio de Educación y Ciencia.

References

1. Y. KANNO, *J. Mater. Sci.* **24** (1989) 2415.
2. H. KOBAYASHI, T. TERASAKI, T. MORI, H. YAMAMURA and T. MITAMURA, *J. Ceram. Soc. Jpn* **99** (1991) 42.
3. T. MORY, H. YAMAMURA, H. KOBAYASHI and T. MITAMURA, *J. Amer. Ceram. Soc.* **75** (1992) 2420.
4. T. ONO, M. KAGAWA and Y. SYONO, *J. Mater. Sci.* **20** (1985) 2483.
5. Y. KANNO and T. SUZUKI, *ibid.* **23** (1988) 3067.
6. *Idem.*, *J. Mater. Sci. Lett.* **7** (1988) 386.
7. S. S. JADA, *J. Mater. Sci. Letters* **9** (1990) 565.
8. B. J. INGEBRETHSEN, E. MATIJEVIĆ and R. E. PARTCH, *J. Colloid Interface Sci.* **95** (1983) 228.
9. A. BALBOA, R. E. PARTCH and E. MATIJEVIĆ, *Colloids Surf.* **27** (1987) 123.
10. R. SALMON and E. MATIJEVIĆ, *Ceram. Inter.* **16** (1990) 157.
11. M. OCAÑA, J. SANZ, T. GONZALEZ-CARREÑO and C. J. SERNA, *J. Amer. Ceram. Soc.* **76** (1993) 2081.
12. M. P. BESLAND, C. GUIZARD, N. HOUNANIAN, A. LARBOT, L. COT, J. SANZ, I. SOBRADOS and M. GREGORKIEWITZ, *ibid.* **113** (1991) 1982.
13. J. C. POUXVIEL and J. P. BOILOT, in "Ultrastructure processing of advanced ceramics", edited by J. D. Mackenzie and D. R. Ulrich (John Wiley, New York, 1988) p. 197.
14. N. B. COLTHUP, L. H. DALAY and S. E. WIBERLEY, "Infrared and raman spectroscopy", Academic Press, San Diego (1990) Chs 5 and 10.
15. M. OCAÑA, V. FORNES and C. J. SERNA, *J. Non-Cryst. Solids* **107** (1989) 187.
16. S. MANN, C. C. PERRY, R. J. P. WILLIAMS, C. A. FYFE, C. G. GOBBI and G. J. KENNEDY, *J. Chem. Soc. Chem Commun.* (1983) 168.
17. M. OCAÑA, V. FORNES and C. J. SERNA, *Ceram. Inter.* **18** (1992) 99.
18. J. S. HARTMAN, R. L. MILLARD and E. R. VANCE, *J. Mater. Sci.* **25** (1990) 2785.
19. Y. KANNO and T. SUZUKI, *J. Mater. Sci. Lett.* **8** (1989) 41.
20. V. S. NAGARAJAN and K. J. RAO, *J. Mater. Sci.* **24** (1989) 2140.
21. M. MAGI, E. LIPPMAA, A. SAMOSON, G. ENGELMARDT and A. R. GRIMMER, *J. Phys. Chem.* **88** (1984) 1518.
22. S. CHAKRABARTI and A. PAUL, *Trans. Indian Ceram. Soc.* **45** (1986) 7.

Received 29 July 1993
and accepted 16 May 1994